Int J Adv Manuf Technol
DOI 10.1007/s00170-016-8696-z

ORIGINAL ARTICLE

The mathematical modelling of the impact of electric (Seebeck) effects on end-milling

Zoltán Pálmai[1] · László Csobod[1]

Received: 25 May 2015 / Accepted: 27 March 2016

Abstract It is a well-known fact that thermoelectric currents, reaching even the scale of ampere, develop during chip formation in the machine-workpiece-tool-chip. The impact of these currents on tool wear in end-milling was examined with a qualitative thermoelectric model, in which wear is described by an autonomous non-linear differential equation. Cutting temperature was measured by a so-called natural thermoelement with C60 and P35 carbide pair, which were submerged into heated Sn bath at validation. The mathematical model can be solved by a numerical method, where the inverse of the differential equation of wear was used. The wear curves determined by calculation fitted well with the measurement results. The results were achieved by cutting experiments using P35 carbide conducted on the C45 quality steel workpiece. It was found that the optimal solution with respect to the wear of the tool behaving as a natural thermal element might be achieved if the current is compensated by an external power source. Based on the model, anomalies might occur in some cases in the thermoelectric system. Further research is necessary to decide if this is only a special characteristic of the model or the model is interpreting really the actual processes.

Keywords Cutting · Electrical current · Mathematical model · Wear · Face-milling

✉ Zoltán Pálmai
palmayz@t-online.hu

László Csobod
veva43@freemail.hu

1 University of Miskolc, Institute of Manufacturing Science, Budapest, Hungary

1 Introduction

In spite of the fact that cutting theory is more than 130 years old, new practical tasks keep coming up in this technology. The solution of these, new problems require the reconsideration of the well-known and accepted theories, which may now be regarded as traditional. It is broadly known that the cutting of metals characterised extreme processes. Strain rate can be even in the magnitude of 10^4 s^{-1}. The temperature of around 1000 °C may develop in the machine-workpiece-tool-chip contact zone rather quickly, at a rate of 10^5–10^6 °C s^{-1}. This is followed by cooling at a rate of 10^3–10^4 °C s^{-1} in the surface layer of the workpiece. Based on the impact of these dynamic processes on chip formation [1] and tool degradation [2], this paper aims to analyse the special group of phenomena occurring as a result of the Seebeck effect and the external electrical circuit.

The complexity of thermoelectric processes is well represented by the research findings of Uehara et al. [3]. In order to study complicated electronic processes, they construed an analogous electric model, by the help of which they managed to show that the input of external voltage of various signs and magnitudes into the chip root fundamentally influences the developing whirling currents.

The obviously close connection among mechanical, thermal and electric processes can most practically be followed by the observation of cutting temperature. Several researchers have dealt with the thermal phenomena of cutting [5] since Gottwein published his research findings on the measurement of cutting temperature conducted by means of a tool-workpiece thermoelement [4]. The first really profound measurements that are published were performed 30 years later by Küsters [6], who studied the temperature developing on the cutting tool using the so-called thermocouple method.

Published online: 21 April 2016

It was highlighted that various electric currents develop among the machine, the tool, the workpiece and the chip during cutting (Fig. 1). Measurement results, according to which the strength of these currents is in the magnitude of ampere, were also published. It was shown by detailed examinations that there is no even temperature distribution on the surface of the tool contacting the chip and the workpiece. As a result of this, the temperature measured on the tool by the thermocouple method can be regarded as an average. Consequently, establishing the maximum value is also important in the examination of e.g. diffusion wear. Lowack [7] conducted extensive research regarding this. He isolated the workpiece and the tool from the machine in thermoelement measurements [8]. Understandingly, in the meantime, the assumption arose that these thermocurrents developing on the tool owing to chip formation, whose magnitude, according to Opitz [9], can even reach 5 A, may even influence wear [10]. These early reports described the examination of cases where the thermocurrent influenced the wear mechanism in a complete circuit or while using insulated tools. Ellis and Barrow [11] found a decreased tool life in the case of insulated tools. According to the extensive research carried out by Durov et al. [12], if the electric circuit of the tool-workpiece was broken, the tool life increased significantly to 1.3–2.9, on average to 1.8 of the normal condition.

Shan and Pandley [13] conducted wear and tool life tests to examine this issue by changing the cutting and circuit conditions. It was shown that the effect of insulation depends on cutting parameters and the electric parameters of the machine-tool-workpiece system in a given tool-machine combination. It was verified by experiments that the revolution of the spindle strongly influences the internal electric resistance of the tool machine, which first massively increases, then stabilises. An electric model was developed for the cutting process, which facilitated the qualitative explanation of wear also during the application of external circuit. The conclusion was drawn that the thermoelectric current flowing through the workpiece-tool-chip system generally increases wear, especially when the polarity of the external current on the tool is negative. It is also a fact, however, that isolating the tool from the machine is not always advantageous regarding wear. This could be shown in the case of low-resistance machine tools. It was observed that oxidation plays a significant role in the wear process influenced by electric current [14]. Apart from oxidation, diffusion can also play a significant role in the wear of carbide tools. Diffusion may also be influenced by electric current or its external compensation [15].

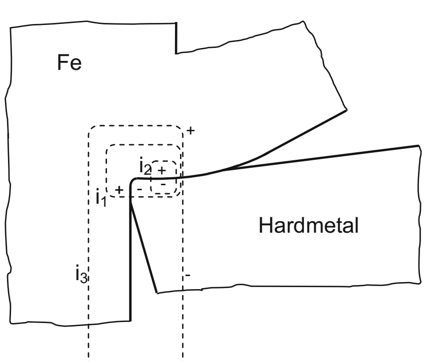

Fig. 1 Currents in the chip root

Measurements simulating various cutting circumstances confirmed the many times controversial findings of former research that the isolating effect of the tool may vary depending on the actual conditions of cutting. In chip formation, the Seebeck effect influences the temperature of the contacting surface of the tool, thus, wear as well. The summary of the experiments is controversial. The use of the insulated tool is beneficial in some cases as opposed to regular cutting. However, sometimes, it is ineffective or harmful. The latter was supported by Uehara et al. [3] with three cutting experiments. They equally found that the isolated tool wears away more quickly than in normal cases when cutting mild steel, steel with medium C content and stainless steel.

The effect of electric field was also examined by the researchers of the wear theory in other areas. Steward et al. [16] showed that electric voltage develops between the tool and the workpiece, which influences wear in the cutting of fibreboard. Examining the friction of aluminium-oxide and cast iron, Wistuba [17] concluded that an internal electric field develops on the contacting and frictional surfaces in the tool-workpiece-chip system, which becomes distorted under the impact of an external electric field. Polarity and the magnitude of external voltage connected to the frictional pairs significantly influence wear rate and even the cutting force. These examinations could also be used for the study of the efficiency of the lubricant [18]. The complex nature of the issue is shown by the fact that new research findings that aim to explore the impact of electric current on wear are regularly published. Gangopadhyay et al. [19] reached the conclusion that wear is smaller if the tool is the cathode through model abrasion and face milling. Moreover, even vibration decreases. Increasing the current also increases the wear.

Tanaka et al. [20] pointed out to an interesting phenomenon. They examined the impact of external current on machinability in free cutting steel manufactured with boron nitride (BN) additive. Their experiments in BN free cutting steel showed that external electric current had a significant impact especially on crater wear as it decreased wear rate. They found a measurable increase depending on polarity at the shear angle and, in connection with this, at the cutting force, while a decrease was seen at passive force. Their examinations are even more remarkable because it is frequent in the cutting of steels like this that a partial or continuous non-metallic layer develops on the surface of the tool contacting the chip or the workpiece [21], which may significantly increase the electric

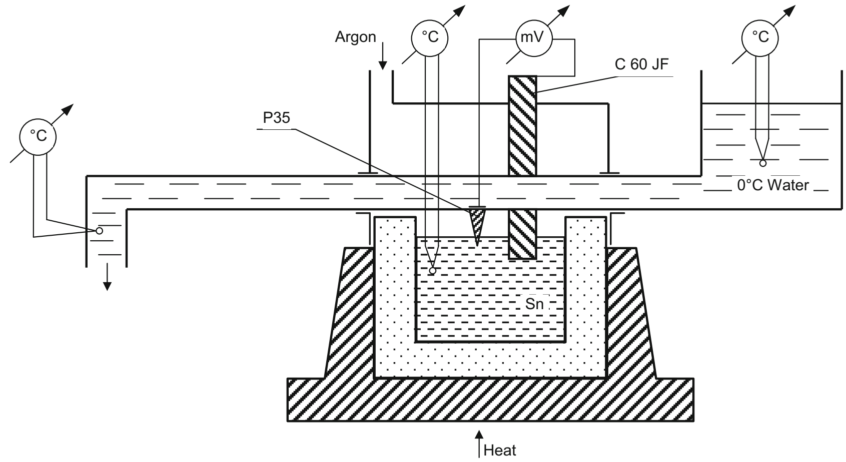

Fig. 2 Measurement arrangement for the calibration of natural thermoelement [24]

resistance on the contacting surfaces, i.e. may fundamentally influence the electric circuits connected to the tool edge.

Besides all these, however, it can be concluded that although the heat impact of the sometimes significant electric current obviously influences the temperature of the contacting surfaces of the tool-workpiece-chip system, a rather moderate interest is found in literature in this topic. This fact leads to the idea of concluding a qualitative analysis based on the experimental findings of Csobod L. [22] regarding the thermoelectric currents developing in the chip root and the impact of externally fed electric current. This paper intends to present a mathematical model that enables the study of electrothermal phenomenon developing in chip formation and the relationships between this phenomenon and tool wear. This paper intends to present a mathematical model that enables the study of electrothermal phenomenon developing in chip formation and the relationships between this phenomenon and tool wear.

2 Cutting temperature and its measurement

The well-known 'classical' formula of cutting temperature is as follows:

$$\Theta_e = \mathrm{C_v v^x} \tag{1}$$

where C_v and x are constants. This then is usually extended by various technological parameters. Actually, the x exponent itself also depends on cutting speed, which can be resolved by using different values in the various temperature ranges [23]. Kalászi [24] also showed that thermovoltage is also influenced by the structural transformation that may occur in contacting materials in the thermoelement measurements of cutting speed, which shall be considered in the evaluation of the results.

Naturally, it is a dynamic process that also depends on time, which, after the initial transient stage, approximates to a constant value in the continuous cutting of a material of constant diameter and this value is usually described with formula (1). In intermittent cutting such as face milling, the transient stage of the process is important, where the application of empirical formula

$$\Theta_e = C_v v^x \exp\left(-\frac{\tau}{t}\right) \tag{2}$$

has proven useful. Here, t means time, and τ is the time constant characteristic of the transient process, e.g. $\tau = 1.95$ μs in the case of steels of moderate C content [23].

The tool-workpiece material pair had to be calibrated as a thermoelement for the measurement of the cutting temperature. The measurement arrangement designed for this purpose is shown in Fig. 2. The hot spot was represented by C60 JF quality steel and carbide marked as P35 dipped in melted Sn as soldering tin within a graphite crucible embedded in a chrome ring, while the cold junction was continuously cooled water of 0 °C temperature. The temperature of the Sn bath could be measured and controlled by external heating. Temperature measurements were conducted by RhPt-Pt thermoelements.

P35 carbide used for calibration contains WC, TiC and TaC and other carbides, which are produced with Co binder material by powder metallurgy. Its composition is shown in Table 1, while that of C60 steel paired to P35 carbide is shown in Table 2.

Table 1 Chemical composition of carbide used in the thermoelement

WC (s%)	TiC (s%)	TaC (s%)	Co (s%)
77	4	8	11

Table 2 Chemical composition of C60 steel used in the thermoelement

Quality	C	Mn	Si	P	S
C60	0.63	0.68	0.26	0.013	0.029

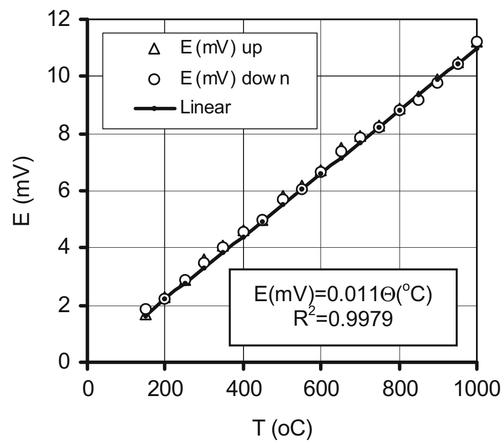

Fig. 3 The calibration curve of the natural thermoelement

The calibration measurement was performed step-by-step at every 50 °C until reaching 1000 °C both during warm-up and cool-down. The results are summarised in Fig. 3. It can be concluded that hysteresis is minimal; the measurement results closely correspond to the regression line representing simple proportionality (R^2 = 0.9979); thus, formula

$$\Theta = c_E E \tag{3}$$

where 1 c_E = 1/0.0111 = 90.1 °C/mV can be regarded as reliable.

In spite of the fact that the listed technological parameters significantly influence thermal conditions on the chip root, and thus, on the tool face, formula (1) has been used for a long time and the related literature is also extensive. Kaminise et al. [25] showed that the thermal conductivity of the tool holding also influences the temperature developing at the edge significantly, while Sun et al. [26] also summarised the results of thermoelement measurements in the milling of Ti alloy with the proven type (1) function. This is regularly applied in finite element method (FEM), like by Lazoglu and Islam [27], who determined cutting temperature by the 3D FEM. This paper is also a good example for the fact that the FEM tools can be valuable supplements to the experimental measurement results when the task is to determine the surface distribution of temperature apart from the average temperature that can be determined by a thermoelement.

Generally, no worn-out but new tools are used when data are collected for the determination of empirical formulas (1) and (2) at the measurement of cutting temperature. According to the findings of many researchers, however, temperature is increasing during the wear of the tool. This phenomenon is broadly discussed in papers. Various reports have been published regarding the question what empirical formula can be used to describe the impact of wear on temperature rise. Colwell [28] pointed out to the mutual connection of flank temperature and flank wear, while Rubinstein [29] summarised the factors influencing cutting temperature, such as flank wear, in a power function, similarly to Kundrák [30], as well as Park and Ulsoy [31].

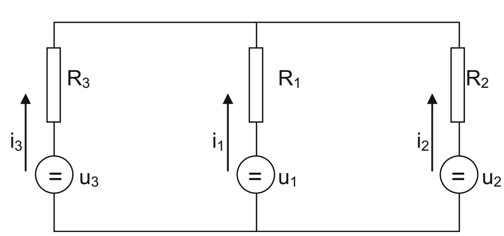

Fig. 4 Circuits in cutting

Table 3 The chemical composition of the workpieces used in milling experiments

Quality	C	Mn	Si	P	S
C45	0.54	0.59	0.23	0.024	0.027
C45 JF	0.53	0.63	0.31	0.017	0.078

Others followed a linear approach of the relationship between wear and temperature, such as Cook [32], who gave a 38 °C temperature increase for 0.1-mm flank wear in the fine machining of austenitic steel. Lowack obtained a value of 33 °C in C steel. Luo et al. [33] regarded the $\Delta\theta$ increment developing on the flank land as a result of wear as proportionate to wear. Barlier et al. [34] reached a similar conclusion. In our case, when a qualitative analysis is the aim, the linear approach is satisfactory and the impact of wear increasing the temperature can be described with the formula

$$\Delta\Theta_w \cong c_w W \tag{4}$$

where W is wear, e.g. VB and c_w are proportionality factors. Based on the data published in cutting literature, the constant of formula (4) in this paper was specified following the measurements of Kodácsy, who sets a value of $c_w \approx 1.2$ °C/μm [35].

3 The thermoelectric model of the chip root

The temperature field on the surface of the cutting tool develops as a combined result of the following three processes.

(a) The fast deformation of the material in the chip root and the friction on the surface of the tool, which can be considered together with the Θ_m mechanical factor.

Table 4 The hardness of the workpieces used in milling experiments (HV10)

Quality	Longitudinal		Crosswise	
C45	203	203	236	209
C45 JF	196	199	209	199

Table 5 The constants of the thermoelectric wear model

c_f	c_{f1} (μm^{-1})	c_E (°C/mV)	c_w (°C/μm)	c_R (μΩ μm)	c_i (°C Ω/A^2)	R_t (mΩ)
0.17	0.001	0.011	1.2	0.03	0.04	0.6

(b) The temperature developing on the surface of the tool increases by $\Delta\Theta_w$ value as a result of wear, which is also connected to the power of the friction force.

(c) The temperature field developing on the contacting surfaces of the workpiece, the tool and the chip creates a special electric potential field on the surface of the tool and whirling currents develop, as shown in Figs. 1 and 2. This results in a further increase $\Delta\Theta_i$ of temperature.

Naturally, these three processes are interrelated, which needs to be taken into account in actual measurements. Thus, the so-called Θ cutting temperature that can be determined by various measurement methods is as follows:

$$\Theta = \Theta_{\mathrm{m}} + \Delta\Theta_{\mathrm{w}} + \Delta\Theta_{\mathrm{i}}. \tag{5}$$

Mostly new, not yet worn tools are used to determine formulas (1) and (2), so the results do not contain the $\Delta\Theta_w$ value. Increment $\Delta\Theta_i$, however, is obviously a part of the Θ value determined by measurement. This is the so-called cutting temperature, which means a specific average value on the working surface of the tool, which makes the rake face maximum warmer and the flank land temperature lower. Thus, a $\Delta\Theta_f$ temperature difference has a meaning for the flank land. So the temperature of the flank land is as follows:

$$\Theta_{\mathrm{f}} \approx \Theta_m + \Delta\Theta_w + \Delta\Theta_i - \Delta\Theta_f. \tag{6}$$

Naturally, formula (2) shall be used instead of (1) for intermittent cutting.

Assumptions for thermo-current calculations:

R_f resistance between the tool flank and the workpiece contact depends on the degree of wear:

$$R_f = \frac{c_R}{W}. \tag{7}$$

It can also be assumed that the temperature difference between the tool face and the flank land can be described by the following linear function:

$$\Delta\Theta_{\mathrm{f}} \approx \mathrm{c_f}\Theta_{\mathrm{f}}(1 + \mathrm{c_{f1}}\mathrm{W}) \tag{8}$$

where c_f and c_{f1} are also constants.

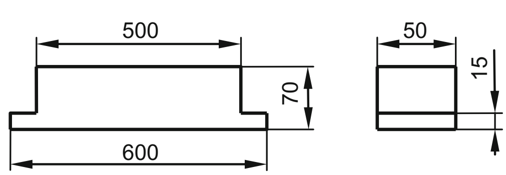

Fig. 5 Experimental workpiece (unit: mm)

Finally, $\Delta\Theta_i$ is the temperature rise that develops due to thermocurrent i_f is as follows:

$$\Delta\Theta_i \cong c_i \frac{{i_1}^2}{R_f} \tag{9}$$

where c_i is constant.

With regard to the qualitative analysis of the impact of electrical circuits, the constants listed above can be estimated from the data that has been published in cutting literature regarding the temperature of the tool flank and the impact of wear on temperature.

According to Fig. 1, the electric field is concentrated in three circuits, and the circuit model is represented by Fig. 4, where $R_1 = R_f$, $R_2 = R_t$, $R_3 = R_m$ and

i_1: current through the rake face and the flank land
i_2: internal current on the rake face
i_3: current through the tool, the chip and the machine

As broadly known, the electromotive force is nearly proportionate to temperature, so if Θ_f is known, u_1 can be

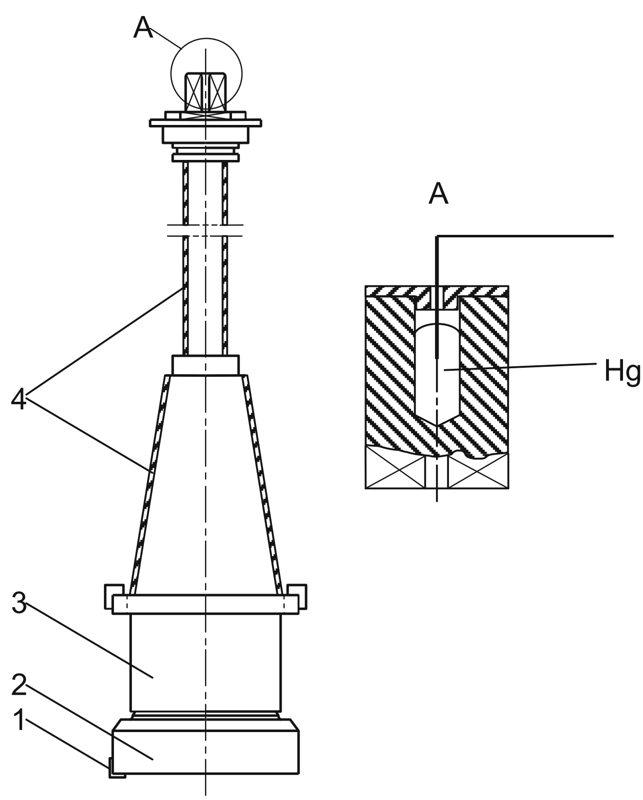

Fig. 6 Insulation of the spindle of the milling cutter converted for experiments (*1*: insert, *2*: milling, *3*: sleeve, *4*: insulating layer)

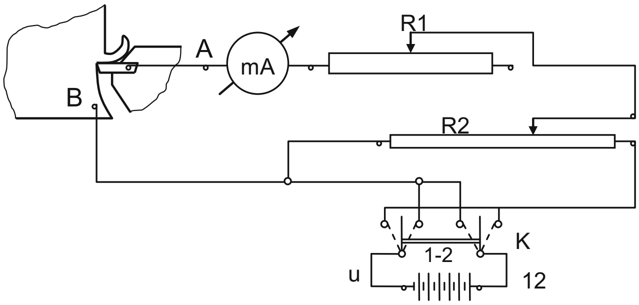

Fig. 7 The connection diagram of the electric current lead through the chip root from an external source

calculated with the following formula:

$$u_1 = E_f = c_E \Theta_\mathrm{f} \tag{10}$$

where c_E is the Seebeck constant regarding the actual material pair, whose value is known from the authors' own measurements [24].

Voltage $u_2 = E_t$ develops on the rake face of Θ temperature, so

$$u_2 = E_t = c_E \Theta \approx c_E \left(\Theta_f + \Delta \Theta_f \right). \tag{11}$$

Voltage marked with u_3 in Fig. 4 only needs to be considered in the special case if an external source of current also works between the tool and the workpiece, as happens in milling experiments presented in this paper. Otherwise $u_3 = 0$.

The strength of the electric current going through the tool flank can be calculated from the circuits shown in Fig. 4. Disregarding the following details:

$$i_1 = \frac{E_f}{c_R + \frac{R_m R_t W}{R_m + R_t}} - \frac{R_m W}{c_R + R_m W} \cdot \frac{E_f + \Delta E}{R_t + \frac{R_m c_R}{c_R + R_m W}} - \frac{R_t W}{c_R + R_t W} \cdot \frac{E_t}{R_m + \frac{c_R R_t}{c_R + R_t W}}. \tag{12}$$

The temperature calculated with these formulas can be used for the calculations of tool wear, for which the following differential equation can be used [35]:

$$\frac{dW}{dt} = \frac{v}{W} \left(A_a + A_{th} \exp - \frac{Q}{R \Theta_f} \right) \tag{13}$$

where v is cutting speed, Q is the activation energy of wear, R is the universal gas constant, and A_a and A_{th} are constants. It can be seen that there is a positive feedback in the relationship of W wear, which is, in our case, VB flank wear, and Θ_f temperature. It is advisable to regard W wear as an independent variable in the numerical solution as this influences R_f resistance (7), $\Delta\Theta_f$ (8) and $\Delta\Theta_i$ (9) heat increment and i_1 current strength (12). Δt will be the dependent variable in the differential version of Eq. (13) in accordance with the following formula:

$$\Delta t = \frac{\Delta W}{dW/dt}, \tag{14}$$

by which function $W(t)$ can then be determined numerically.

4 Cutting experiments with face milling

Materials taken from two steel charges were used in experiments. One of these was a normal C45 steel, and the other was a special deoxidized steel of C45 JF quality, whose chemical compositions are detailed, based on control analysis, in Table 3, while their hardness is included in Tables 4 and 5.

The drawing of the workpiece used during cutting experiments can be seen in Fig. 5. The tool machine used for measurements was a UF221 type horizontal axis milling cutter, on which a vertical axis face-milling cutter was assembled. An insert was put into the tool ($\gamma_o = 6°$, $\kappa = 70°$, $\varepsilon_r = 90°$, P35 carbide). The technology was as follows: feed $f = 0.105$ mm/edge, depth of cut $a = 2.5$ mm, without cooling, cutting speed

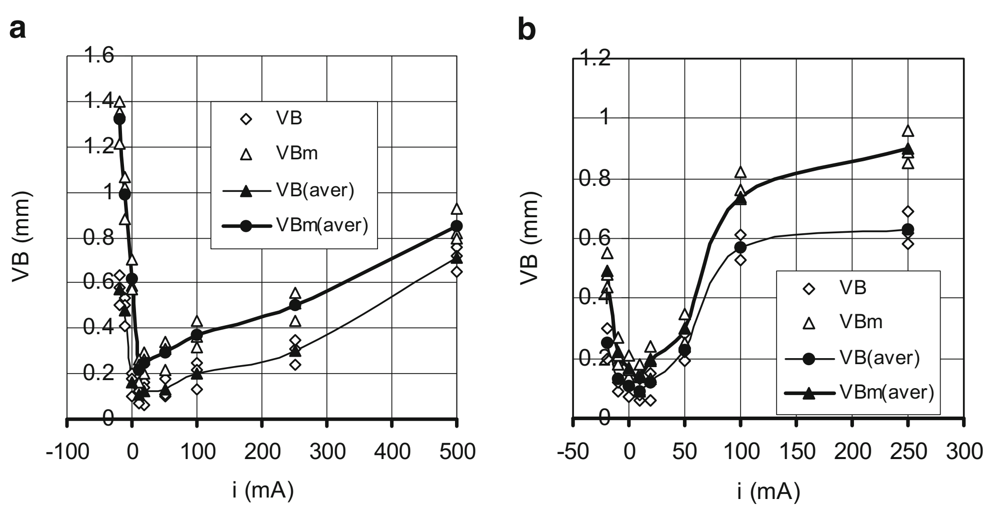

Fig. 8 Tool wear in various external currents ($t = 4.15$ min, average: *black circle*, *black triangle*). **a** Material: steel C45. **b** Material: steel C45JF

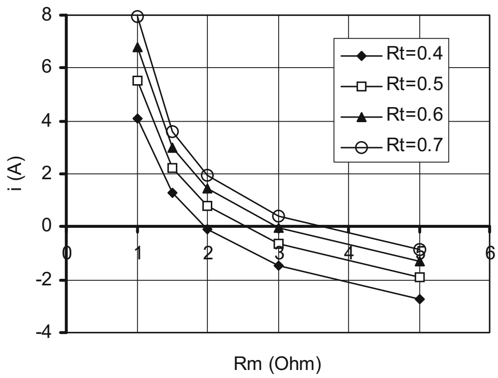

Fig. 9 Current strength i as a function of R_m and R_t (mΩ) resistances ($E_m = 0$, VB = 200 μm)

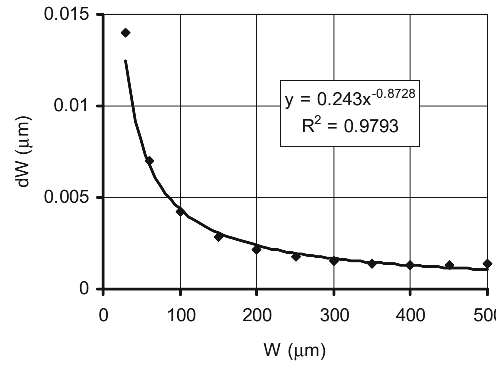

Fig. 11 dW(W) increase of wear in a single cutting cycle ($E_m = 0$, $R_m = 2$ mΩ, $R_t = 0.6$ mΩ, $A_a = 8.10^{-6}$μm, $A_{th} = 200$ μm, $Q = 152$ kJ/mol, $\tau = 1.95$ ms)

236, 298 and 371 m/min. Most examinations were performed with a speed of $v = 298$ m/min, where the tool was cutting for $t_o = 10{,}057$ ms during one rotation of the milling cutter. The VB average and VB_m maximum flank wear of the tool were measured by the ocular micrometre of a profile microscope. The duration of cutting in the examination of various external voltage effects was 4.15-min effective cutting during the cutting of five layers of $L = 500$ mm, which meant $N = 23{,}728$ cutting cycles.

The axis of the face milling machine was isolated from the remaining parts of the machine as shown in Fig. 6. The electric lead out was arranged through the Hg in the upper end of the spindle, into which the connecting electric cable was immersed during rotation, so various voltages could be applied to the tool from a battery (12 V) (Fig. 7).

The soldered copper cable directly connecting the cutting insert with the spindle, also marked in the picture, ensured the elimination of the electric resistance between the connecting parts. The examinations were conducted in several stages with allowing the system to ‘rest’, so that the temperature increase of the connecting points should not distort the results.

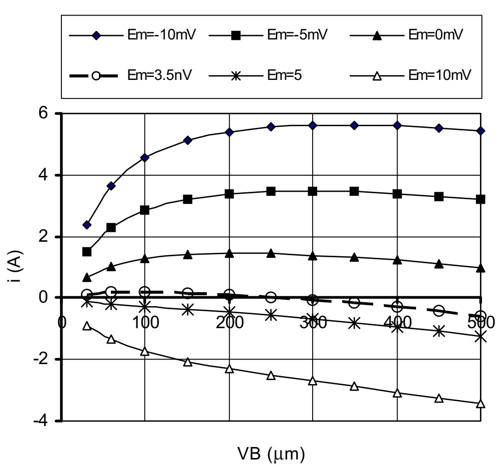

Fig. 10 Calculated i_1 current as a function of wear at various external E_m voltages ($W = \mathrm{VB}$, $R_m = 2$ mΩ)

The electric connection diagram of the measurements is shown in Fig. 7, where resistances $R1$ and $R2$ facilitated the control of power, while switch K the setting of the direction of current. External voltage u_3 shown in Fig. 4 is generated between points A and B as displayed by Fig. 7, while the circuit elements to the right of these points jointly constitute the external generator shown in Fig. 4.

The external current lead through the chip root this way was superimposed to current generated by thermovoltage; thus, it was added to it or was compensated by it, depending on its direction. The results of cutting experiments are shown in Fig. 8. It can be seen that the current lead through the contacting points of the chip root significantly influenced tool wear, and the optimum value specified based on tool wear is nearly at the same external current in both measurement series.

5 Calculations using the thermoelectric model

The thermoelectric model presented in Section 3 facilitates the qualitative analysis of the electric current developing as a result of the Seebeck effect. Naturally, this current influences cutting temperature. Constants summarised in Table 2 were used for calculations. Using the data of the publication quoted in Section 2, the constants were determined in a way that the calculation results are in line with the wear measurement results.

An important feature of intermittent cutting is the dynamic change of temperature, which is described by function (2) and which is repeated at each revolution of the milling cutter in the experiments. As temperature and electrical current are in close

Table 6 Tool wear values measured at various cutting speeds ($E_m = 0$)

v (m/min)	236	298	371
tc (min)	2.135	4.17	0.67
VB_m (μm)	80	150	70
VB_{kalc} (μm)	94.1	146.5	68.3

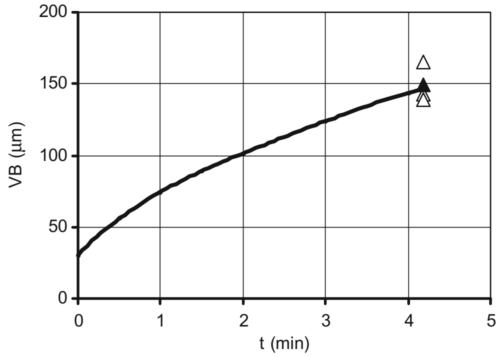

Fig. 12 Adjusting the calculated wear curve to the measurement results ($E_m = 0$, $R_m = 2$ mΩ, $R_t = 0.6$ mΩ, $A_a = 8.10^{-6}$µm, $A_{th} = 200$ µm, $Q = 152$ kJ/mol, $\tau = 1.95$ ms, average: *black triangle*)

relationship, the latter changes periodically. Therefore, it is important to consider that the values shown in there refer to the end of the cutting cycle when evaluating Figs. 9 and 10.

Figure 9 represents what connection there is between the R_m resistance of the tool machine, the R_t resistance developing on the tool and the thermocurrent in the normal case of cutting without external voltage. The value $R_m = 2$ mΩ and $R_t = 0.6$ mΩ was chosen for further calculations. This way, we get the current curves shown in Fig. 10 as a function of external voltage E_m. It is interesting to observe that the current most probably changes sign, i.e. between the values of $E_m = 0$ and 5 mV direction during tool wear.

The tool in each rotation cuts through the approximately circle-shaped arc which is determined by the B width of the workpiece and the D diameter of the milling cutter during face milling. Wear can be calculated with Eq. (13), where it must be considered that temperature θ is also the function of time based on formula (2). The calculation can be simplified using the circumstance that a cutting cycle is nearly a thousand times shorter than the expected tool life. ΔW wear can be calculated with Eq. (13) for a cutting cycle in various $W = 30$, 60, 100… µm statuses, regarded as constant. An empirical ΔW = ΔW(W) function can be prepared from the increment of ΔW wear obtained for a cutting cycle at various W values,

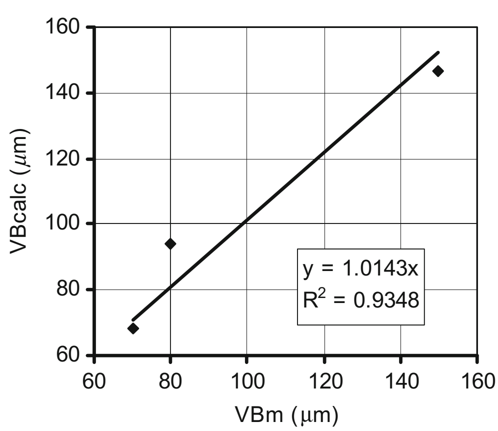

Fig. 13 The comparison of measured VB_m and calculated VB_{calc} tool wear

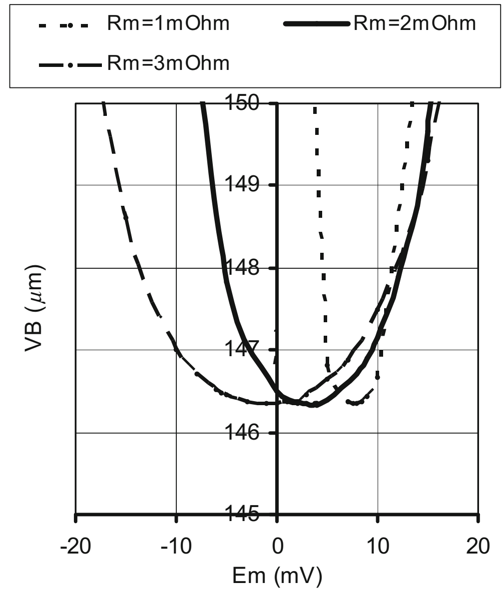

Fig. 14 Tool wear at various external E_m voltages ($t = 4.15$ min)

regarded as constants. By the help of this, also considering the increasing wear during milling, the actual wear curve can be calculated.

The actual cutting time at the ith cycle in $v = 298$ m/min speed milling is as follows:

$$t(\text{min}) = it_{f0} = 0,01057\frac{i}{60} \tag{15}$$

while wear is

$$W_i = \Delta W(W) + W_{i\text{-}1}. \tag{16}$$

It seemed practical to choose the simple power function

$$\Delta W = AW^B \tag{17}$$

Zfor the generation of the ΔW(W) function, where A and B can be determined from ΔW_j wears calculated for individual

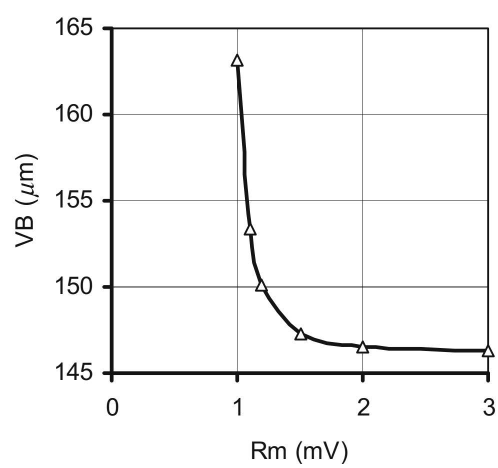

Fig. 15 The effect of the R_m internal resistance of the tool machine ($E_m = 0$, $t = 4.15$ min)

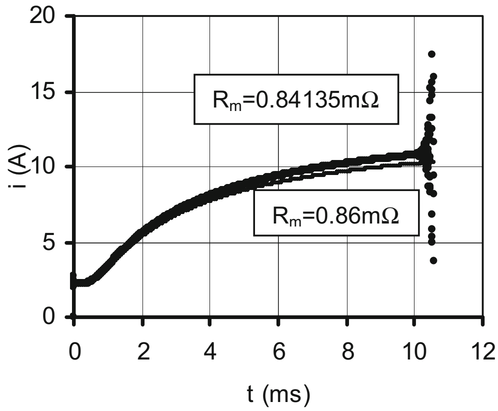

Fig. 16 The change of current strength during the cutting cycle ($E_m=0$, VB = 300 μm)

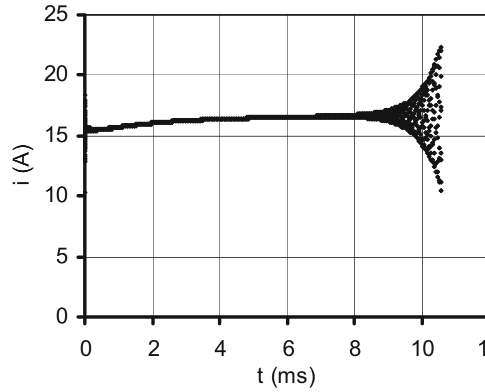

Fig. 18 The change of current strength during the cutting cycle ($E_m=-34.6$ mV, $R_m=2$ mΩ, VB = 300 μm)

W_j = constant values. For example, Fig. 11 shows how the ΔW(W) curve obtained this way corresponds to the to the ΔW_j results calculated at W_j wear levels, regarded as constant. The $R^2=0.9793$ Pearson number can be regarded as quite good.

By the help of function (17), differential Eq. (13) regarding tool wear can be used, which must be connected to formula (14). Now, the Δt value must be calculated step-by-step as a function of wear increasing by ΔW in the numerical solution; thus, the $W(t)$ wear curve can be obtained. Using wear measured at $v=298$ m/min speed (Table 6), the calculated wear curve can be seen in Fig. 12.

Wear examinations were also conducted with two other speeds, whose results are also shown in Table 6. The effect of speed v must be considered in two places in the calculation: in wear Eq. (13) and in formula (3) at constant C_v. The latter can be done in formula (2) by the help of exponent x, which was determined by the empirical $x=0.27$ value [36].

The results calculated for the three speeds and compared with measurement results are shown in Fig. 13. The relationship is not close but this is not surprising knowing the usually large scatter of cutting examination results and the small amount of data. However, the thermoelectric model is suitable for e.g. the qualitative reproduction of the effect measured by experiments with the application of external voltage (Fig. 8). Figure 14 shows at the three values of R_m how tool wear depends on external voltage E_m in the parameters that can be seen in Fig. 12. Two conclusions can be drawn on this basis. On the one hand, it is striking that the minimal flank wear is independent of internal resistance R_m of the machine; on the other hand, this small value occurs at different E_m external voltages depending on the internal resistance. It is interesting to note that the model shows a rather fast wear in the case of very small electric resistance of the machine, i.e. in a state close to short circuit. Figure 15 represents this in a case where there is no external voltage supply, i.e. the tool operates under normal cutting circumstances.

6 The anomalies of model calculations in intermittent cutting

Studying the cutting process during a single rotation of the milling cutter, the calculations also revealed interesting anomalies of the developing electric current. Then the effect of these obviously appears in the cutting temperature, consequently, in the tool wear, as well. In this paper, only the special behaviours of the i current strength are discussed in two groups of the phenomena.

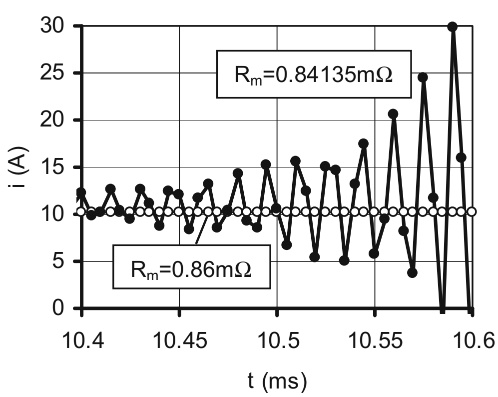

Fig. 17 The curve seen in Fig. 16 in an enlarged time scale

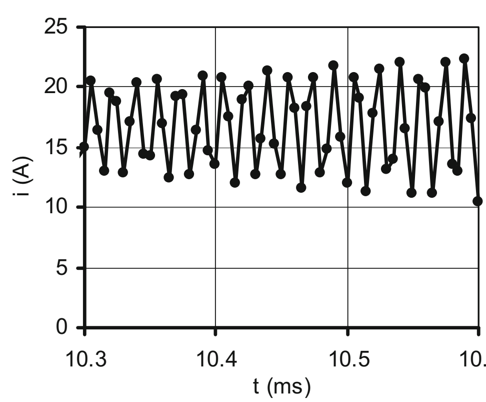

Fig. 19 The curve seen in Fig. 19 in an enlarged time scale

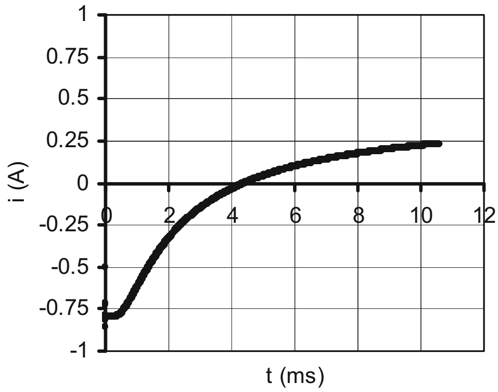

Fig. 20 Current increase in the case of $E_m = 2.8$ mV ($R_m = 2$ mΩ, VB = 300 μm)

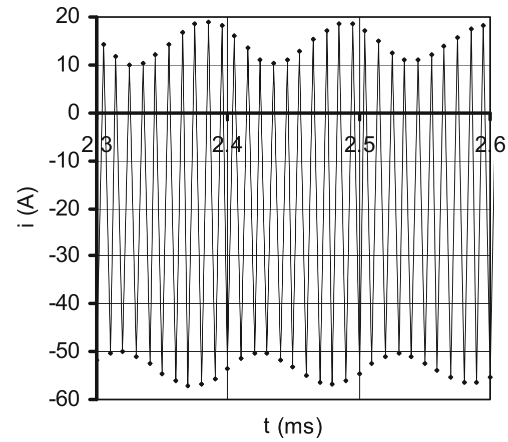

Fig. 22 An enlarged detail of Fig. 21 ($E_m = 64.3$ mV)

Using the constants of the thermoelectric model summarised in Table 5, interesting results can be obtained at $E_m = 0$, i.e. under normal cutting circumstances if the internal resistance R_m of the tool machine is small. Assuming $R_m = 0.86$ mΩ and in $W = \mathrm{VB} = 300$ μm wear condition, the increase of electric current strength determined by calculation can be seen in Fig. 16, in which only the peaks of the wave line are shown so that the results can be evaluated more easily. If an even smaller machine resistance is assumed, the current strength will fluctuate at the end of the cutting cycle. In Fig. 16, empty circle signs mark the current developing in the case of $R_m = 0.86$ mΩ, while solid circles represent the fluctuating current strength at $R_m = 0.84135$ mΩ resistance. Unlike Fig. 16, the continuous wave curve of current strength can be seen here. Based on Fig. 17, we can conclude that oscillation frequency of the current does not equal to time scale used in the calculation. The former is 0.016 ms, while the latter is 0.005 ms and their relationship is 3.2. This is relevant because we must emphasise the possibility that the anomalies which may be seen below are not the characteristics of the chip formation itself but arise from the mathematical model.

A similar phenomenon can be observed when $R_m = 2$ mΩ, but the external voltage is $E_m < 0$. Based on Fig. 18, the current starts to fluctuate with increasing amplitude towards the end of the cutting cycle in this case, as well. The details of the process are shown by Fig. 19, according to which the cycle time of fluctuation equals to what can be established based on Fig. 17.

Increasing the value of E_m in the negative direction, the instability increases and commences sooner during the cutting cycle and the amplitude also increases.

If external E_m voltage is increased in the positive direction, the direction of the current also changes. Interestingly, this happens e.g. at $E_m = 2.8$ mV ($R_m = 2$ mΩ, VB = 300 μm) during the cutting cycle (Fig. 20). If E_m is further increased, a different type of phenomenon can be seen. As it is shown in Fig. 21, the current curve changes significantly. The curve that represents the effect of several variations of external voltage E_m also indicates only the peaks of the fluctuating current. The curve rises slightly and monotonously at $E_m = 50$ mV, but at higher values of external voltage ($E_m = 53$ mV), it starts with a periodical fluctuation, whose amplitude then decreases and the fluctuation of the current ceases. However, the fluctuation of current strength is maintained until the end at even higher external voltages ($E_m = 55$ mV); moreover, it can even turn chaotic. In the case of $E_m = 64.3$ mV, a multi-cycle oscillation develops, with a decreasing then temporarily increasing amplitude; finally, a one-cycle wave arises. These processes seem to be independent of the time scale applied in the calculation, as it can be seen from Fig. 22.

Fig. 21 The change of current strength during the cutting cycle ($R_m = 2$ mΩ, VB = 300 μm)

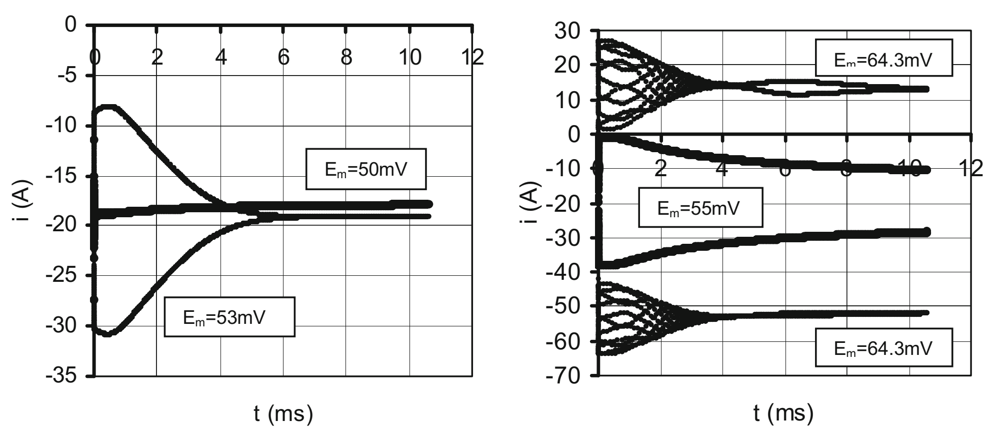

7 Summary

Thermoelectric currents, reaching even the scale of ampere, develop in the machine-workpiece-tool-chip system during cutting as a result of the Seebeck effect. The heat effect of a current of this magnitude may have a significant impact on the temperature of the chip root. Its measurement was conducted with a so-called natural thermoelement, in which the thermocouple was a C60 quality steel workpiece and a P35 carbide tool. The thermocouple was immersed in heated Sn bath during calibration.

A qualitative thermoelectric model was elaborated to determine the electric current that flows through the contacting surface of the workpiece and the tool. Wear is described with a non-linear differential equation in this model, and the study of the current lead into the system from an external voltage source became possible. The mathematical model was solved with a numerical method using the inverse of the differential equation of wear. The wear curve determined by calculation fits in with the measured result. It could be concluded based on the milling experiments performed with P35 carbide on C45 quality steel workpieces that it is optimal regarding the wear of the tool behaving as a natural thermoelement if the thermal current is compensated with an external power source.

The results of the calculations can be summarised as follows: significant currents may flow in the chip root, which also depend on the tool wear, and this dependence is mutual. According to the calculation prepared based on the qualitative model and cutting experiments, the tool wear is also minimal if the thermal current is compensated by an external source of current. It can be concluded that anomalies may be observed in the behaviour of the system based on the mathematical model.

Based on the available data, it cannot be determined with absolute certainty if this phenomenon is the result of the mathematical model itself or a specific feature of the electrothermal processes occurring in the chip root. It is a fact that the cycle time of the wave equals with the time scale applied for the calculation in the case of regular alternation; however, this is not so in chaotic conditions. On the other hand, it must also be noted that the model was prepared considering the actual temperature conditions developing in the chip root, which refers to the possibility that the anomaly occurs in the technological process. Further research is necessary to find the answers for the open questions.

Acknowledgments The authors greatly appreciate the (financial) support of the National Research, Development and Innovation Office—NKFIH (No. of Agreement: OTKA K 116876). This research was carried out in the framework of the Center of Excellence of Innovative Engineering Design and Technologies at the University of Miskolc.

References

1. Pálmai Z (2013) Egy lokális deformációval megvalósuló fémtechnológia matematikai modellezése. Anyagok Világa 2:1–33
2. Pálmai Z (2014) A forgácsolószerszámok kopásának matematikai modellezése felületi degradációjuk vizsgálata alapján. Anyagok Világa 1:8–50
3. Uehara K, Sakurai M, Ikeda T (1992) On the problem of thermoelectric current in metal cutting. Ann CIRP 41(1):75–78
4. Gottwein K (1926) Temperature of the cutting edge in turning as dependent on the form of chip cross-section. Maschinenbau 5:187
5. Solaja V, Hughes H (1958/59) Some electrical phenomena in metal cutting. Wear 2: 311–314
6. Küsters KJ. Temperaturen im Schneidkeil spanender Werkzeuge, Dissertation 1956. Technische Hochschule, Aachen
7. Lovack H (1967) Temperaturen an Hartmetalldrehwerkzeugen bei der Sthalzerspanung. Dissertation. Technische Hochschule, Aachen
8. Lowack H (1968) Temperaturen an Hartmetallwerkzeugen bei der Stahlzerspanung. Industrie Anzeiger 90 Nr. 34. v. 26.4: 709
9. Opitz H (1957) About wear on cutting tools. Proc. Conf. Lubrication and Wear, Inst. Mech. Engrs., London, pp. 664
10. Simpson FF, Russel RW (1957) Influence of magnetic field and passage of electrical currents on the deterioration of ball bearings. Proc. Conf. Lubrication and Wear, Inst. Mech. Engrs., London, pp. 477
11. Ellis J, Barrow G (1969) Tool wear in metal cutting and its relationship with the thermo-electric circuit. Ann CIRP 17:39–50
12. Dubrov JC, Nikolaeva GC, Filolenko VC (1973) K voprosu o fizitheskoi vliania thermoelektritheskih iavlenia na processa trenia i rezania metallov. Izdatlestvo Nauka, Moskow
13. Shan HS, Pandey PC (1975) Wear of cutting tools: thermo-electric effects. Wear 32:167–179
14. Shan HS, Pandey PC (1976) Oxidation and wear behaviour of carbide tools. Wear 37:69–75
15. Bredell LJ (1983) The influence of thermo electric current on the wear of tungsten carbide tools. In: Science of hard materials. Springer, p 723–734
16. Steward HA, Srinivasan S, Stiffler AK, Miller DB (1994) Electrical discharge when machining medium-density fiberboard and tool wear. Tribol Int 27(5):343–348
17. Wistuba W (1997) The effect of an external electric field on the operation of an aluminium oxide–cast iron sliding contact joint. Wear 208:113–117
18. Wistuba W (1997) A phenomenon of triboelectrization in aluminium oxide–polytetrafluoroethylene sliding contact joint operating under reduced lubrication conditions. Wear 208:118–124
19. Gangopadhyay A, Barber G, Zhaob H (2006) Tool wear reduction through an externally applied electric current. Wear 260:549–553
20. Tanaka R, Yougchuan L, Akira H, Ueda T (2009) Influence of additional electric current on machinability of BN free-machining steel in turning. J Adv Mech Des Syst Manuf 3(2):171–178
21. Pálmai Z (1984) Formation of non-metallic protective layers on high-speed steel tools. Metal Technol 11:34–37
22. Csobod L (1983) A forgácsolás hőjelenségeinek vizsgálata szakaszos forgácsleválasztásnál, a termoelektromos jelenség felhasználásával. Disszertáció. Miskolci Egyetem
23. Pálmai Z (1987) Cutting temperature in intermittend cutting. Int J Mach Tool Manuf 27(2):261–274
24. Kalászi I (1966) A phenomenon leading to an error in measuring the cutting temperatures by the tool/work method. Int J Prod Res 4: 329–335
25. Kaminise AK, Guimaraes G, de Silva MB (2014) Development of a tool–work thermocouple calibration system with physical compensation to study the influence of tool-holder. Int J Adv Manuf Technol. doi:10.1007/s00170-014-5898-0

26. Sun Y, Sun J, Li J, Xiong Q (2014) An experimental investigation of the influence of cutting parameters on cutting temperature in milling Ti6Al4V by applying semi-artificial thermocouple. Int J Adv Manuf Technol 70:765–773
27. Lazoglu I, Islam C (2012) Modeling of 3D temperature fields for oblique machining. CIRP Ann Manuf Technol 61:127–130
28. Colwell LV (1975) Cutting temperature versus tool wear. Ann CIRP 24(1):73–76
29. Rubenstein C (1976) An analysis of tool life based on flank-face wear. J Eng Ind: 221–232
30. Kundrák J (1996) The scientific principles of increasing the effectiveness of inner surfaces' cutting with CBN tools. Harkov, p 368
31. Park J-J, Ulsoy AG (1993) On-line flank wear estimation using an adaptive observer and computer vision. J Eng Ind Trans ASME 115:30–43
32. Cook NH (1973) Tool wear and tool life. J Eng Ind Trans ASME: 931–938
33. Luo X, Cheng K, Holt R, Liu X (2005) Modeling flank wear of carbide tool insert in metal cutting. Wear 259:1235–1240
34. Barlier C, Lescalier C, Mosian A (1997) Continuous flank wear measurement of turning tools by integrated microthermocouple. Ann CIRP 46(1):35–38
35. Kodácsy J (2010) Nem publikált mérések Kecskeméti Főiskola
36. Pálmai Z (2013) Proposal for a new theoretical model of the cutting tool's flank wear. Wear 303:437–445